

Do cylinders exhibit a cubatic phase?

Ronald Blaak, Daan Frenkel and Bela M. Mulder
*FOM Institute for Atomic and Molecular Physics, Kruislaan 407,
1098 SJ Amsterdam, The Netherlands.*

(October 6, 2018)

Abstract

We investigate the possibility that freely rotating cylinders with an aspect ratio $L/D = 0.9$ exhibit a cubatic phase similar to the one found for a system of cut-spheres. We present theoretical arguments why a cubatic phase might occur in this particular system. Monte Carlo simulations do not confirm the existence of a cubatic phase for cylinders. However, they do reveal an unexpected phase behavior between the isotropic and crystalline phase.

I. INTRODUCTION

The phase behavior of apparently simple systems can be surprisingly rich. In 1957 Alder and Wainwright reported the first simulations of a system of hard spheres¹. They showed that, upon increasing density, this system exhibits a phase transition from an homogeneous liquid to a crystalline FCC phase, even though there is no attractive interaction.

An almost equally simple system that exhibits an even richer phase behavior, is the hard spherocylinder model, that was introduced by Onsager in 1949². Onsager used this model to show that hard, elongated, rodlike particles must undergo a transition from the isotropic to nematic phase. Subsequently, computer simulations, revealed that a smectic A and two different crystalline phases can exist³⁻⁵, depending on the aspect ratio. Recent extensions of the Onsager theory to higher densities and smaller aspect ratios can account for these novel phases⁶⁻⁹.

In order to study the behavior of disklike objects Eppenga and Frenkel performed simulations of a system of infinitely thin disks¹⁰. By construction, the packing fraction of such a system is zero. As a consequence, after aligning the particles, the system can easily be compressed, nevertheless, the nematic to columnar transition for this system has been studied¹¹. A different model for disklike object was proposed by Veerman and Frenkel¹². They used cut-spheres, which are obtained by symmetrical slicing off the polar caps of a sphere. As a function of the length over diameter ratio of these particles, they connect the infinitely thin discs with the spheres. Surprisingly, cut-spheres with an aspect ratio of about 0.2, appear to exhibit an orientationally ordered phase with a cubic symmetry, which is called the cubatic phase, even though these particles themselves have a cylindrical symmetry.

In this article we investigate a possible explanation of the existence of the cubatic phase for cut-spheres. To this end we study, by computer simulation, a system of freely rotating cylinders. In Sec. II we present a theoretical basis for looking at cylinders. In Sec. III

we elucidate some of the techniques used in our Monte Carlo simulation. This involves the overlap criterion of these particles and an additional type of move that we used in our simulations. In Sec. IV we show the main results from the computer simulations and discuss the unexpected behavior of cylinders between the isotropic and crystalline phase. The symmetry of this new phase is analyzed in Sec. V. In Sec. VI we determine the coexistence between the isotropic liquid and the crystalline phase by means of a free energy calculation. In Sec. VII we discuss the main results and give some suggestions for future research.

II. CUBATIC PHASE

The cubatic phase is a long-range orientationally ordered phase without any positional order of the particles. In a uniaxial nematic phase the particles, e.g. rods, tend to align along a single preferred direction. In a biaxial phase for single component systems, e.g. biaxial ellipsoids¹³, the different molecular axes of the particles align in three different orthogonal directions. In the special case that these three directions are also equivalent, in the sense that each molecular axis is with equal probability in any of the three directions, we obtain an orientationally ordered phase with cubic symmetry. In the absence of translational order this is the elusive cubatic phase.

Evidence for this cubatic phase was first found in computer simulations of cut-spheres with an aspect ratio $L/D = 0.2$ ¹². However, subsequent theoretical work indicates that particles, consisting of three perpendicular, elongated rods of approximately the same length, at least in the Onsager limit of infinite aspect ratios, should also form this cubatic phase^{14,15}. Experimentally, however, this cubatic phase has never been observed.

Figure 1 shows a snapshot of the cubatic phase of cut-spheres. The figure suggests that the disklike objects tend to form stacks of several particles in an approximately cylindrical shape. These cylindrical clusters are then arranged in such a way that there is an overall cubatic order. As a first attempt to explain the cubatic phase for cut-spheres we will attempt to describe the system on the level of these aggregates. This is a simplification, because the stacks in Fig. 1 are obviously not perfect cylinders but polydisperse in both length and shape. Yet, in what follows, we model this system as a collection of monodisperse, hard cylinders.

In order to select the optimal aspect ratio that might give rise to a cubatic phase, we first consider the excluded volume of two cylinders. Onsager already gave an expression for the excluded volume \mathcal{E} of two arbitrary cylinders with lengths L_i and diameters D_i ²

$$\begin{aligned} \mathcal{E}(\gamma) = & \frac{\pi}{4}D_1D_2(D_1 + D_2) \sin \gamma + L_1L_2(D_1 + D_2) \sin \gamma \\ & + L_1 \left(\frac{\pi}{4}D_1^2 + D_1D_2E(\sin \gamma) + \frac{\pi}{4}D_2^2|\cos \gamma| \right) \\ & + L_2 \left(\frac{\pi}{4}D_2^2 + D_1D_2E(\sin \gamma) + \frac{\pi}{4}D_1^2|\cos \gamma| \right) \end{aligned} \quad (1)$$

where γ is the angle between the two main axes of the cylinders and $E(x)$ is the complete elliptical integral of the second kind.

In Fig. 2 we have plotted the excluded volume of two identical cylinders as function of the angle γ , for several aspect ratios. To facilitate comparison we normalized the excluded volume to unity for perpendicular orientations. Note that for the aspect ratios, zero

and infinity, $\mathcal{E}(\gamma)$ reduces to the same monotonically increasing function. This reflects the tendency of strongly anisotropic particles to align. For an aspect ratio of the order unity, however, we see that the maximum excluded volume is found between the parallel and perpendicular orientation. In fact, for the latter two orientations the excluded volume exhibits a minimum, although the deepest minimum always corresponds to a parallel orientation.

In a cubatic phase both parallel and perpendicular orientations should be present. However, it is logical to look for that aspect ratio that minimizes the relative difference between both minima. The fact that parallel orientations lead to a smaller excluded volume, and are therefore favored, could be compensated by the fact that forming a cubatic phase would lead to a higher orientational entropy. This is because particles in a cubatic phase can be aligned in three different directions instead of a single one as in the case of only parallel orientations. In Fig. 3 we have plotted the ratio of the perpendicular and parallel orientation as a function of the aspect ratio. The minimum of the curve occurs for the aspect ratio $L/D = \sqrt{\pi}/2 \approx 0.886$, where the excluded volume of perpendicular orientations is only 1.133 times larger than that of parallel orientations.

III. SIMULATION

In our search for a possible cubatic phase for hard cylinders, we performed Monte Carlo simulations of a system of freely rotating, hard cylinders with an aspect ratio $L/D = 0.9$.

A. Overlap criterion

In¹⁶ an overview is given of the most widely used overlap criteria for convex hard particles. The one for cylinders is only outlined. It consists out of three steps.

1. *spherocylinder overlap*: For the first step we replace the cylinders by spherocylinders by adding hemispheres on both sides of the cylinders. We then compute the closest distance between the spherocylinders. If the spherocylinders do not overlap the cylinders will not either. If the spherocylinders do overlap we can only conclude that the cylinders overlap if the vector of shortest distance intersects both cylindrical parts.
2. *disk-disk overlap*: If the last condition is not satisfied we need to continue with the second step. In this step we check whether there is an overlap of the flat faces of the cylinders.
3. *disk-cylinder overlap*: If no overlap is found in the second step, and the spherocylinders in the first step did overlap we need to proceed with the third step, which is the most time-consuming one. We have to check whether one of the flat faces of a cylinder overlaps with the cylindrical hull of the other cylinder.

According to¹⁶ this last problem reduces to calculating overlaps between two planar ellipses, and hence is a special case of the overlap between two ellipsoids. It is this last step which is the most difficult.

For ellipsoids there exist two different criteria to determine whether there is an overlap or not. The first is due to Vieillard-Baron¹⁷ and the second due to Perram and Wertheim¹⁸.

Both criteria determine whether there exists an overlap without calculating any points which both particles have in common. But although the intersection of the plane in which the flat face lies with the cylindrical hull of the other particle is an ellipse, the ellipse is not necessarily complete. This happens if the plane also intersects with one of the flat faces of the second cylinder. In that case we need to check whether there is an overlap with the incomplete ellipse.

The alternative route is to look at the problem as the overlap between a flat face of one cylinder with a sequence of circles of the second particle. This results in a fourth order polynomial equation and can in principle be solved analytically. The main problem with this approach is that during simulations it will result in severe problems, and not always find the correct outcome. The reason for this is that the coefficients of the polynomial equation are inversely proportional to the sine of the angle between the particles. Therefore the coefficients can differ by orders of magnitudes, which makes it hard to solve and not always accurate.

The method we applied for the last step in the overlap criterion therefore is a direct minimization of the distance between a point on the edge of the first cylinder and a point on the axis of the second cylinder. Although it is slower, it has proven to be very reliable.

B. Flip-move

In Monte Carlo simulations we wish to sample the complete configuration-space in an efficient way. In our Monte Carlo simulations we keep the number of particles N , the pressure P and the temperature T are fixed. We performed several distinct type of trial moves. We try to translate and rotate particles by a small amount. In addition we perform volume changing moves in order to equilibrate the density under the applied pressure. For details about these standard techniques, we refer to¹⁹.

At high densities, we can only perform relatively small trial moves, because otherwise the acceptance of the moves becomes negligibly small. However, this may create a kinetic barrier to equilibrate a cubatic phase, in which particles are parallel or perpendicular to each other, while intermediate orientations are less likely due to steric hindering. It is difficult to achieve a rotation of a cylinder over 90° by a succession of small rotational moves.

In order to sample the configuration space of this system more efficiently, we introduce an extra trial move: the flip move. Rather than waiting for the rare reorientation of a cylinder over 90° through a succession of small angular jumps, we attempt to rotate it directly to a perpendicular orientation. The flip-move is a proper Monte Carlo move that satisfies detailed balance. By construction it is such, that it does not break the symmetry of an isotropic phase. In the case of short cylinders this trial move is surprisingly effective.

To illustrate this we have shown in Fig. 4 three steps of the continuous rotation of a short cylinder in a dense ordered phase. The first picture shows that for parallel particles there is still some space to move. However, if the cylinder in the middle is rotated by 45° , its dimension in the plane changes causing it to overlap with neighboring particles. As the rotation continues the excluded volume of the cylinder decreases again. By including the flip-move we bypass the unfavored intermediate state.

During our simulations on average 1 out of every 10 rotations will be an attempt to flip a particle. To this end, we select at random an orientation in the plane perpendicular to

the direction of the particle and accept it if there is no overlap in the new situation. The acceptance of this move depends of course strongly on the aspect ratio and density, but can be as large as 5%, even in a crystalline phase.

C. Nature of crystalline phase

There are several relevant crystalline structures to study for a system of cylinders with an aspect ratio of order unity. The highest possible density in a system of cylinders is reached when all cylinders are perfectly aligned in a close-packed structure with the particles ordered in hexagonal layers. This leads to a maximum packing fraction $\phi = \pi/\sqrt{12}$.

In the case of spheres there are many different possible ways to stack the layers to form a regular crystal. The simplest stackings are the face centered cubic (FCC) and hexagonal close-packed (HCP) structure. In both structures, the close-packed layers are shifted with respect of each other, such that the centers of mass in one layer are above the holes in the layer below. This leads to three different layer positions labeled by A, B and C. The FCC crystal corresponds to ABC stacking, while ABAB stacking is characteristic for the HCP crystal²⁰.

In the case of a densely packed crystal of cylinders, there is an infinity of possible stackings positions, provided that the close-packed planes are flat. However away from close packing, the system will prefer a situation where the layers are stacked in an AAA fashion. Other stackings are not stable and will relax to this structure.

If the cylinders are not confined to close-packed planes, the AAA crystal phase could deform in a columnar phase. In this phase the cylinders are organized in a hexagonal array of columns. However, there is no long-range correlation between the longitudinal displacement of different columns.

Another crystalline phase that is possibly relevant is the simple cubic crystal, in which the orientation distribution of the cylinders has the same symmetry as the lattice. Although this phase cannot be close packed, it allows us prepare a structure that has the same orientational symmetry as a cubatic phase. This is achieved by aligning the cylinders at random with any of the three axes of the crystal.

IV. SIMULATION RESULTS

Constant NPT-MC simulations were performed on a system of 720 particles. Long runs were needed to collect good statistics (typically 10^5 trial moves per particle excluding equilibration). On average a volume change was attempted N times less frequently than the simple particle moves. One in every ten trial rotations was a flip-move.

In our NPT simulations of the solid phase, we allowed the shape of the simulation box to change to an arbitrary parallelepiped rather than keeping it rectangular. Such a move was first used by Parrinello and Rahman²¹⁻²³ in MD simulations and later by Najafabadi and Yip in MC simulations²⁴. Allowing for shape changes is only useful in crystalline structures, because then the presence of the crystal structure acts as a restoring force and will ensure that the box shape cannot become extremely anisotropic. In a liquid phase, extreme deformations could occur, because a natural restoring force does not exist.

The resulting equation of state is shown in Fig. 5, where we plotted the reduced pressure $\beta P v$ versus the packing fraction ϕ , where v is the volume of a single cylinder and $\beta = 1/(k_B T)$ the inverse temperature. The two branches are obtained by compressing a low-density liquid phase and expanding a high-density AAA-crystal. The equation of state provides no indication that a cubatic phase, or any other intermediate phase, exists.

If we start with a crystalline phase in which the hexagonal layers are stacked in a different fashion, for instance ABC, the layers will swiftly slide with respect to each other to form an AAA-stacking. Occasionally, we find that the columns shift with respect to each other, but this is probably a finite size effect, rather than an indication of a columnar phase.

We can also start from a simple cubic crystal in which the particles are either regularly or randomly aligned with respect to the three axes of the crystal. This phase is also not stable but tends to transform into an the AAA-crystal. It is observed that this sometimes leads to two AAA-crystals with different orientations. However, it is likely that, given enough time, the grain boundary that has formed will anneal out.

The flip-move is extremely effective. Even for a packing fraction $\phi = 0.7$ one out of every 1000 attempted flips is accepted. For $\phi = 0.65$ this is already one out of every 100 and increases to about 7% near the transition to the isotropic phase. A simulation, without using this flip-move, showed that at $\phi = 0.65$ particles can achieve a flip via a continuous rotation, but this occurs with a very low probability, only once in a simulation of 10^5 sweeps. Therefore the introduction of the flip-move speeds up this slow ‘dynamical’ process enormously, leading to a faster convergence to equilibrium.

In order to get an impression what these systems look like, three snapshots are shown in Fig. 6. The first snapshot shows a high-density isotropic phase. The second represents a high-density, almost perfect AAA-crystal at a packing fraction $\phi = 0.684$, with one orientational defect. The third and most interesting snapshot is obtained at the low-density side of the crystalline branch. This is the place where, the cubatic phase would be observed if it existed. The phase that we observe appears to be neither isotropic nor perfectly crystalline. A stunning feature of this phase is the fact that the shape of the simulation box changes from a rectangular shape at high densities to a non-orthogonal shape in the intermediate region. As the symmetry of the structure differs from both the high density solid and the low density liquid, we must classify it as a separate phase. Since the equation of state shows no hint of a first-order phase transition, the novel phase is probably joined to the crystalline phase by either a continuous or weakly first-order transition and is found at packing fractions between $\phi \approx 0.55$ and $\phi \approx 0.65$.

V. SYMMETRY OF THE INTERMEDIATE PHASE

In order to analyze the nature of the intermediate phase we discuss the translational and orientational order separately. To characterize the positional order we use the bond orientational order parameters Q_l used by Steinhardt *et al.*²⁵,

$$Q_l = \left\langle \left(\sum_m |C_{l,m}(\vec{r})|^2 \right)^{\frac{1}{2}} \right\rangle, \quad (2)$$

where we determine the polar angles of the vector \vec{r} connecting neighboring particles. Only particles within a distance of twice the length of the particles are used.

The bond orientational order parameters for $l = 4, 6$ and 8 are shown in Fig. 7. As can be seen from the figure, the behavior of these order parameters does not indicate any sudden structural phase transition. Figure 8 shows the projections of the centers of mass of the particles close to melting ($\phi = 0.567$). The top view shows clearly the hexagonal structure, indicating the presence of columns. The side view shows that columns lie within planes.

We use the system at packing fraction $\phi = 0.567$ to illustrate the orientational order in the phase near the transition. In Fig. 9 we plot all orientations of the particles on a unit sphere. It is clear that particles are oriented either along a main axis or in a plane perpendicular to that direction.

In order to detect the orientational order we calculate the following matrix

$$\mathbf{Q} = \frac{1}{N} \sum_{i=1}^N \left(\frac{3}{2} \hat{u}_i \hat{u}_i - \frac{1}{2} \mathbf{I} \right), \quad (3)$$

where \hat{u}_i is the director of a particle and N is the total number of particles. The nematic order parameter \bar{P}_2 is defined as the average value of the maximum eigenvalue of the matrix \mathbf{Q} and the nematic direction as the corresponding eigenvector. Furthermore we evaluate the order parameters I_l , defined by

$$I_l = \left\langle \left(\sum_m C_{l,m} C_{l,m}^* \right)^{\frac{1}{2}} \right\rangle. \quad (4)$$

These order parameters are defined in terms of the modified spherical harmonics $C_{l,m}$, and are frame independent. I_2 is related to the nematic order parameter. But whereas the nematic order parameter \bar{P}_2 measures uniaxial order only, I_2 measures the combination of uniaxial and biaxial order. The order parameter I_4 is also able to measure uniaxial order, but now via P_4 , and biaxial order. In addition, however, it is also able to measure cubatic order. It is therefore a non-zero I_4 combined with the absence of nematic order, and thus a zero valued I_2 , which would indicate the presence of cubatic order in the system.

Both order parameters, \bar{P}_2 and I_4 , are shown in Fig. 10. The non-zero value of \bar{P}_2 on the complete crystalline branch, indicates that there is a single preferred or average direction in the system. It turns out that this direction is along the direction of the columns of the crystal. For low density crystals, however, the value of \bar{P}_2 is small and comparable to the nematic order close to the isotropic-nematic phase transition. This is explained by the fact that particles are either aligned along the columns or perpendicular to them. For lower densities more particles will have there direction perpendicular to the columns. It is not favorable to have a direction in between the two extreme orientations.

In order to detect the orientational order in the plane perpendicular to the columns, we finally consider the average of the functions $\sin l\varphi$, where the angles φ of the directors of the particles are measured in the plane perpendicular to the average direction obtained from (3)

$$C_l = \langle |C_{l,l}| \rangle. \quad (5)$$

These order parameters are also shown in Fig. 10, and indicate that there is a small, 4-fold symmetry present. This is caused by the preference of particles in a layer to be either parallel or perpendicular. The 4-fold symmetry is, however, in conflict with the 6-fold symmetry of the crystal. These conflicting symmetries are probably the reason of the non-orthogonal unit cell.

In Fig. 11 we show the radial distribution function $g(r)$ and the orientational correlation functions $g_l(r)$ for $l = 2$ and 4, that are defined by

$$g_l(r) = \langle P_l(\hat{u}(0) \cdot \hat{u}(r)) \rangle, \quad (6)$$

where P_l is the l th Legendre polynomial and $\hat{u}(r)$ is a unit vector along the axis of a particle at distance r from the reference particle. These correlation functions are a measure of the range of the orientational order. As can be seen from Fig 11, $g_2(r)$ and $g_4(r)$ are finite throughout the complete simulation box. Although the correlation function $g_4(r)$ is measuring a combination of nematic-like and cubatic-like order, the magnitude of $g_4(r)$ compared to that of $g_2(r)$ indicates that the cubatic-like order is dominant. This is different from a normal nematic phase where $g_2(r)$ is larger than $g_4(r)$.

Finally we show in Fig. 12 the density correlation functions $h_\alpha(r)$ defined by

$$h_\alpha(r) = \langle \rho(0)\rho(r) \rangle / \rho^2, \quad (7)$$

where the distance r is measured along the α direction and in units of the simulation box length. The functions h_x and h_y show distinct features, as could be expected from the projections shown in Fig. 8, and the number of peaks correspond to the number of layers present in that direction. In the z direction a weak modulation is observed, although the peaks of the function h_z are less pronounced. This can partly be understood if one realizes that the fluctuations in the positions along the columns can be of the order of 20% of the effective size of the particles in that direction. These fluctuations are even enhanced by the fact that particles are oriented along and perpendicular to the columns, but the effective size in both cases is different. For the system sizes that we studied, the density modulation in the z direction persists over the entire simulation box. However, we cannot rule out the possibility that the modulation will decay in even larger systems. If this were the case, the system would, in fact, be in a columnar phase.

In summary, in our simulations we find evidence for an intermediate phase with 3D-crystalline structure in which hexagonal layers are stacked in an AAA fashion. The orientations of the particles are coupled to the crystal axes and are either along the columns or within the layers, in which case they have a slight 4-fold symmetry. Neither the equation of state, nor the order parameters show any indication that there is a first order phase transition along the crystal branch to the perfect, aligned crystal. The novel phase is found at packing fractions between $\phi \approx 0.55$ and $\phi \approx 0.65$, although this upper boundary is somewhat arbitrary as we found no clear phase transition. Above this boundary, however, less than 1% of the particles is misaligned with the crystal.

VI. FREE ENERGY CALCULATION

In order to determine the coexistence between the isotropic liquid and the ordered phase we have to find points on the equation of state with equal pressure and chemical potential.

To this end we need to determine the free energy. By performing a thermodynamic integration along the equation of state we can evaluate the free energies up to a constant. This integration is only allowed if there is no first order transition along the integration path, which in our case is true because all evidence indicates that the transition on the crystal branch is continuous.

In order to proceed we need to determine one reference point on either branch of the equation of state. In the isotropic phase this is easy because we can use the ideal gas as a reference state

$$F(\rho) = F_{id}(\rho) + \int_0^\rho d\rho' \frac{P(\rho') - \rho'}{\rho'^2}. \quad (8)$$

For the crystal phase we use as a reference system an Einstein crystal with the same structure²⁶, which in our case is a perfectly aligned AAA-crystal. We connect the two systems by a one parameter Hamiltonian which consists of two parts, the coupling of the particles to their equilibrium lattice positions and the alignment for the orientations

$$H_\lambda = \lambda \sum_i (\vec{r}_i - \vec{r}_i^0)^2 + \lambda \sum_i \sin^2(\theta_i), \quad (9)$$

where λ is the coupling parameter, \vec{r}_i^0 are the lattice positions, \vec{r}_i the positions of the particles and θ_i are respectively the orientation of the particles with respect to the preferred direction. By slowly increasing the value of λ the system will order according to the imposed field. We used here the same coupling parameter for both fields, but one can also use different values to do the orientational and positional ordering separately.

The free system with $\lambda = 0$ can be related to the Einstein crystal for which $\lambda \gg 1$ by

$$\frac{\beta F(\rho)}{N} = \frac{\beta F_{ein}(\lambda_{max})}{N} - \int_0^{\lambda_{max}} d\lambda \langle \delta r^2 \rangle_\lambda - \int_0^{\lambda_{max}} d\lambda \langle \sin^2 \theta \rangle_\lambda - \frac{\log V}{N}, \quad (10)$$

where $\langle \delta r^2 \rangle_\lambda$ is the mean square displacement and $\langle \sin^2 \theta \rangle_\lambda$ the average sine squared of the angle between the directors of the particles and the direction of the alignment field. The last term corrects for the fact that the center of mass during this simulation needs to be fixed. The value of λ_{max} is chosen such that a system using this Hamiltonian only will not cause any overlaps in the system. For that limit we can derive the value of the free energy of the Einstein crystal²⁷

$$\beta F_{ein}(\lambda) = -\frac{1}{2} \log N - \frac{3}{2}(N-1) \log\left(\frac{\pi}{\beta\lambda}\right) - N \log\left(\frac{2\pi}{\beta\lambda}\right). \quad (11)$$

In the case that overlaps do occur, it is possible to correct for this²⁶. By simulating the system for different values of λ the integrals in (10) can be evaluated numerically. In order to minimize the error we used the Gauss-Legendre quadrature.

The coexistence is obtained is at packing fraction $\phi = 0.515 \pm 0.003$ for the isotropic and $\phi = 0.552 \pm 0.006$ for the crystalline structure, at a pressure $\beta P v_0 = 8.76 \pm 0.08$ (Fig. 5).

VII. DISCUSSION

Our study of the hard cylinder system was inspired by the possibility that it might exhibit a cubatic phase. We have presented Monte Carlo simulation for cylinders with an aspect ratio $L/D = 0.9$. In the standard NPT-simulations we introduced the flip-move, which rotates a particle directly to a perpendicular orientation. Furthermore we allowed the box shape to change to an arbitrary parallelepiped to facilitate equilibration of the crystalline phase.

At high pressures the system is found in an AAA-crystal with particles aligned along the direction perpendicular to the layers. By lowering the pressure, particles reorient, deform the perfect crystal and form an intermediate phase in which the 6-fold symmetry of the crystal is slightly distorted and only very weak layering can be observed. The orientations are either along the columns or perpendicular to them. Towards the phase transition to the isotropic liquid, a weak, but significant, 4-fold orientational order in plane develops. There is no indication that this structural phase transition is first order. The phase coexistence between the isotropic and crystal phase was determined at packing fractions $\phi = 0.515$ in the isotropic phase and $\phi = 0.552$ for the crystal phase.

Our simulations did not reveal a true cubatic phase. In fact, a theoretical analysis of this system²⁸ suggests that the isotropic to cubatic phase transition occurs at a density beyond that of the isotropic to nematic phase transition. This theory predicts that the isotropic to cubatic transition would take place at a packing fraction $\phi \approx 0.80$. However, at this density positional order cannot be neglected and should be incorporated in the theoretical description.

The present results suggest that it is an oversimplification to represent stacks of cut-spheres by monodisperse hard cylinders. As can be seen in Fig. 1, the stacks are polydisperse in length and shape. It might be possible that a cubatic phase is stabilized by introducing polydispersity to the system. However, such a study is outside the scope of the present paper.

ACKNOWLEDGMENTS

We thank Martin Bates for a critical reading of the manuscript. The work of the FOM Institute is part of the research program of FOM and is made possible by financial support from the Netherlands Organization for Scientific Research (NWO).

REFERENCES

- ¹ B. J. Alder and T. E. Wainwright, *J. Chem. Phys.* **27**, 1208 (1957).
- ² L. Onsager, *Ann. (N.Y.) Acad. Sci.* **51**, 627 (1949).
- ³ A. Stroobants, H. N. W. Lekkerkerker, and D. Frenkel, *Phys. Rev. Lett.* **57**, 1452 (1986).
- ⁴ P. Bolhuis and D. Frenkel, *J. Chem. Phys.* **106**, 666 (1997).
- ⁵ D. Frenkel, H. N. W. Lekkerkerker, and A. Stroobants, *Nature* **332**, 822 (1988).
- ⁶ A. M. Somoza and P. Tarazona, *Phys. Rev. A* **41**, 965 (1990).
- ⁷ A. Poniewierski and R. Holyst, *Phys. Rev. A* **41**, 6871 (1990).
- ⁸ H. Graf, H. Löwen, and M. Schmidt, *Prog. Colloid Polym. Sci.* **104**, 177 (1997).
- ⁹ H. Graf and H. Löwen, *Phys. Rev. E* **59**, 1932 (1999).
- ¹⁰ R. Eppenga and D. Frenkel, *Mol. Phys.* **52**, 1303 (1984).
- ¹¹ M. A. Bates and D. Frenkel, *Phys. Rev. E* **57**, 4824 (1998).
- ¹² J. A. C. Veerman and D. Frenkel, *Phys. Rev. A* **45**, 5632 (1992).
- ¹³ P. J. Camp and M. P. Allen, *J. Chem. Phys.* **106**, 6681 (1997).
- ¹⁴ D. Frenkel, in *Liquids, Freezing and Glass Transition*, edited by J. P. Hansen, D. Levesque, and J. Zinn-Justin (North-Holland, Amsterdam, 1991), pp. 689–762.
- ¹⁵ R. Blaak and B. M. Mulder, *Phys. Rev. E* **58**, 5873 (1998).
- ¹⁶ M. P. Allen, G. T. Evans, D. Frenkel, and B. M. Mulder, *Adv. Chem. Phys.* **86**, 1 (1993).
- ¹⁷ J. Vieillard-Baron, *J. Chem. Phys.* **56**, 4729 (1972).
- ¹⁸ J. W. Perram and M. S. Wertheim, *J. Comp. Phys.* **58**, 409 (1985).
- ¹⁹ D. Frenkel and B. Smit, *Understanding Molecular Simulation. From Algorithms to Applications* (Academic Press, Boston, 1996).
- ²⁰ C. Kittel, *Introduction to Solid State Physics*, 6th ed. (John Wiley & Sons, New York, 1986).
- ²¹ M. Parrinello and A. Rahman, *Phys. Rev. Lett.* **45**, 1196 (1980).
- ²² M. Parrinello and A. Rahman, *J. Appl. Phys.* **52**, 7182 (1981).
- ²³ M. Parrinello and A. Rahman, *J. Chem. Phys.* **76**, 2662 (1982).
- ²⁴ R. Najafabadi and S. Yip, *Scripta Metall.* **17**, 1199 (1983).
- ²⁵ P. J. Steinhardt, D. R. Nelson, and M. Ronchetti, *Phys. Rev. B* **28**, 784 (1983).
- ²⁶ D. Frenkel and A. J. C. Ladd, *J. Chem. Phys.* **81**, 3188 (1984).
- ²⁷ J. M. Polson, E. Trizac, and D. Frenkel, (Unpublished).
- ²⁸ R. Blaak, Ph.D. thesis, University of Utrecht, 1997.

FIGURE CAPTIONS

1. Snapshot of the cubatic phase for cut-spheres.
2. The excluded volume of two identical cylinders as function of the mutual angle γ for different aspect ratios $L/D = 0$ and ∞ (solid), 1 (dashed), 2 (long dashed) and 10 (dotted-dashed). The excluded volume is normalized to unity for perpendicular orientations.
3. The ratio of excluded volume for perpendicular and parallel orientations as a function of the aspect ratio of the cylinders. The minimum is found for $L/D = \sqrt{\pi}/2$.
4. Top view of a hexagonal structure for cylinders with aspect ratio of order unity. The left figure shows the aligned case and the middle figure the case when the particle is perpendicular to a layer. The right figure shows an intermediate orientation causing overlap.
5. The equation of state of cylinders with $L/D = 0.9$ for the isotropic (\circ) and crystal (\diamond) phase. The reduced pressure βPV_0 , where v_0 is the volume of a single particle, is plotted versus the packing fraction ϕ . The point of coexistence between the isotropic and crystal branch are connected by the solid line.
6. Three snap shots from simulations, corresponding to isotropic (top left), high density crystal (top right) and ordered phase near the transition (bottom). The packing fractions for these phases are respectively 0.478, 0.684 and 0.567.
7. The bond orientational order parameters $Q_4(\circ)$, $Q_6(\diamond)$ and $Q_8(\square)$ as function of the packing fraction in the ordered phase.
8. The projections of a configuration at packing fraction $\phi = 0.567$. The top view (top) shows the hexagonal pattern of the columns which can be seen from the side (under left). In the front view (right under) planes are more difficult to observe.
9. The orientational distribution for a configuration at $\phi = 0.567$.
10. The orientational order parameters as function of the packing fraction in the ordered phase. The nematic (\circ), cubatic (\diamond) and C_4 (\square) order parameters are non-zero, C_2 (\triangle) and C_6 (∇) are negligible small.
11. The radial distribution function $g(r)$ (\circ) and the orientational correlation functions $g_2(r)$ (\square) and $g_4(r)$ (\diamond) as a function of the distance r measured in units of the diameter of the cylinders at $\phi = 0.567$.
12. The correlation functions $h_\alpha(r)$ as function of the distance along the axis and measured in units of the box length at $\phi = 0.567$. h_x (solid) and h_y (dotted-dashed) clearly indicate the presence of layers in the x respectively y direction. Although h_z (dashed) has less pronounced peaks, also here layering is visible.

FIGURES

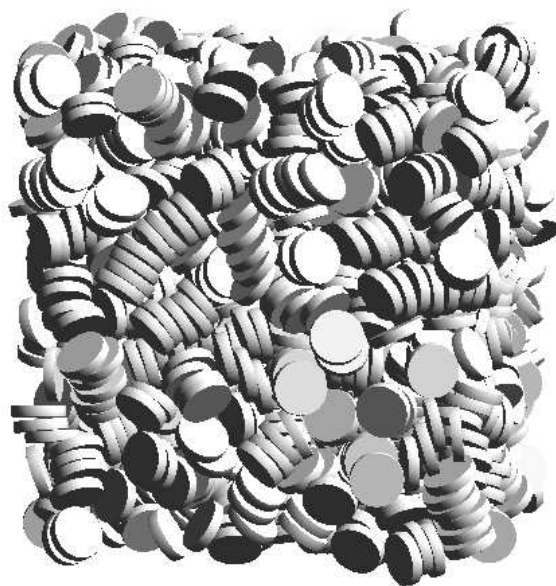


FIG. 1. R. Blaak, Journal of Chemical Physics

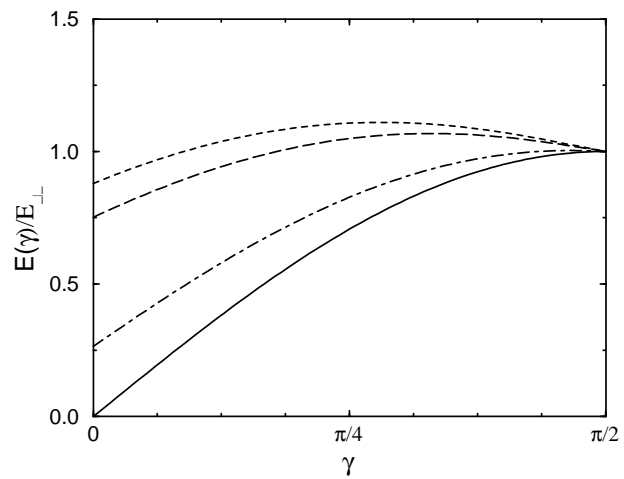


FIG. 2. R. Blaak, Journal of Chemical Physics

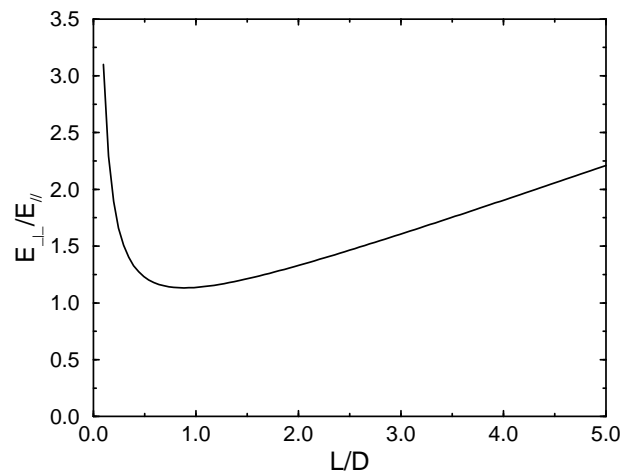


FIG. 3. R. Blaak, Journal of Chemical Physics

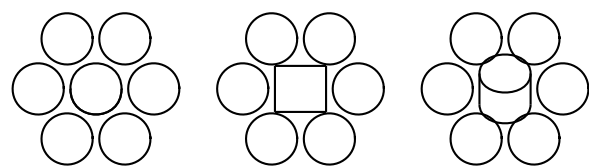


FIG. 4. R. Blaak, Journal of Chemical Physics

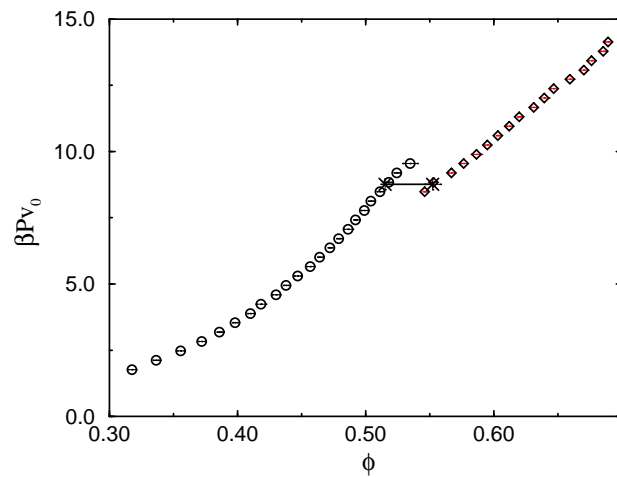


FIG. 5. R. Blaak, Journal of Chemical Physics

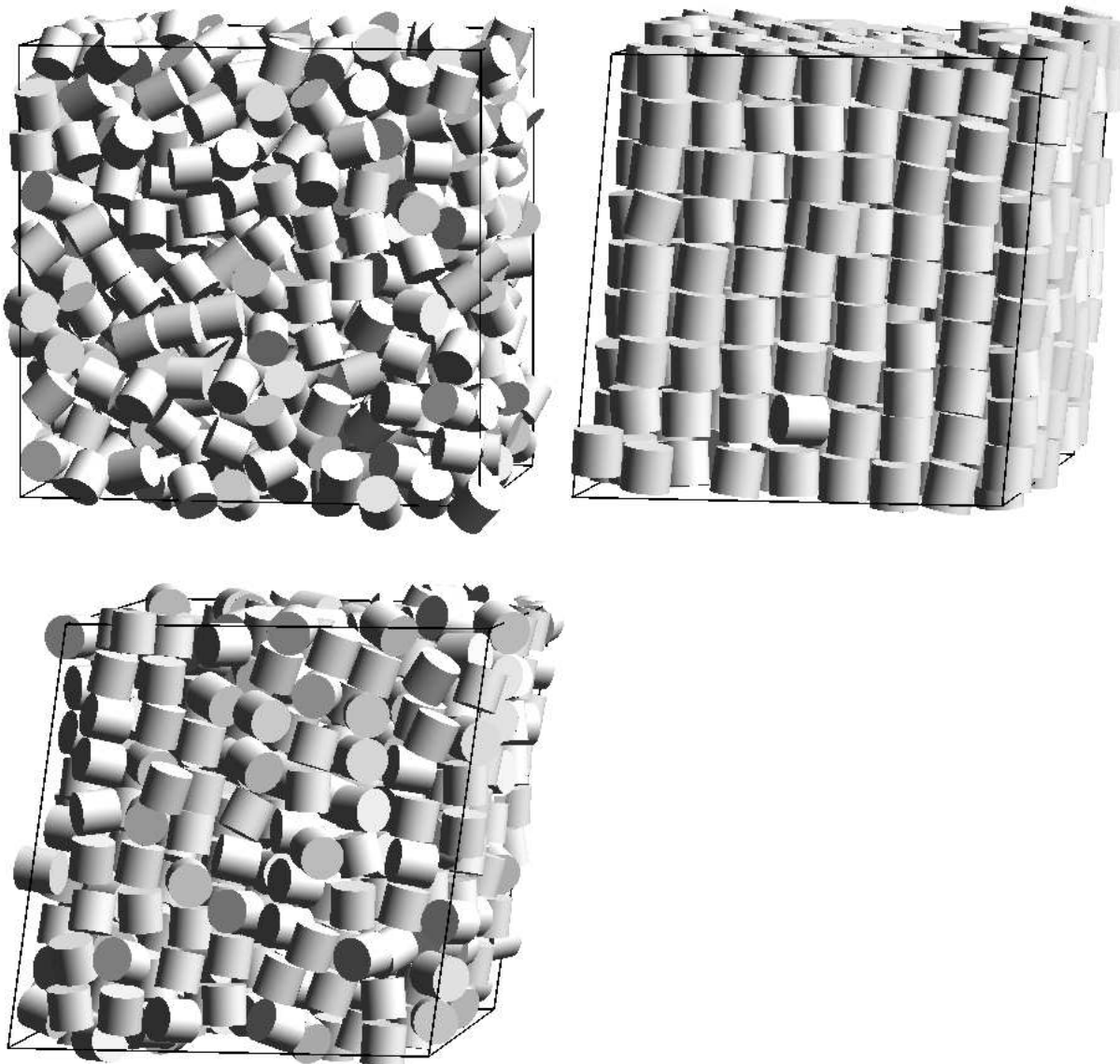


FIG. 6. R. Blaak, Journal of Chemical Physics

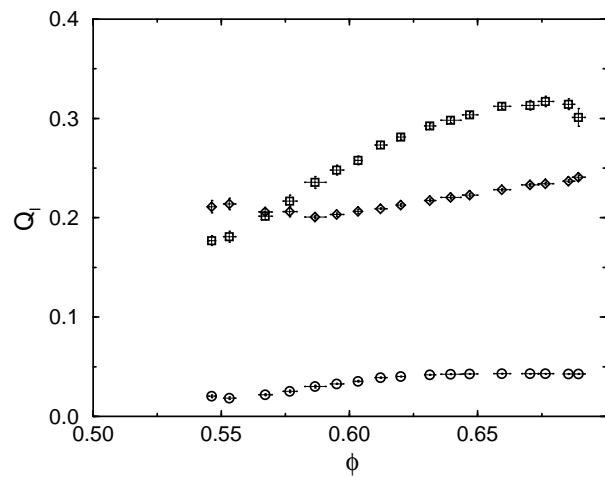


FIG. 7. R. Blaak, Journal of Chemical Physics

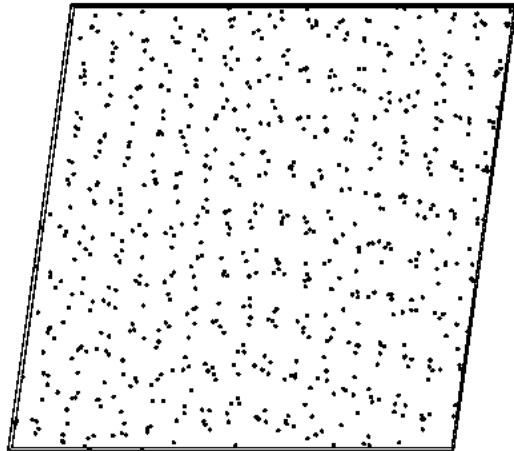
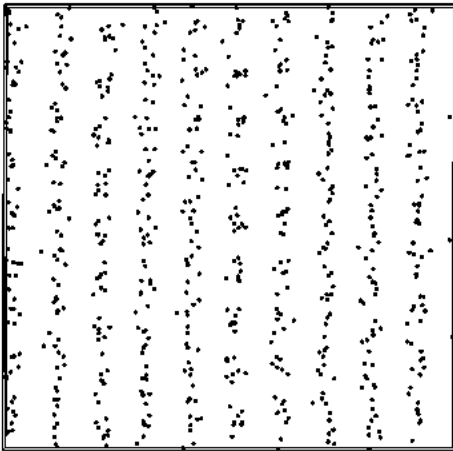
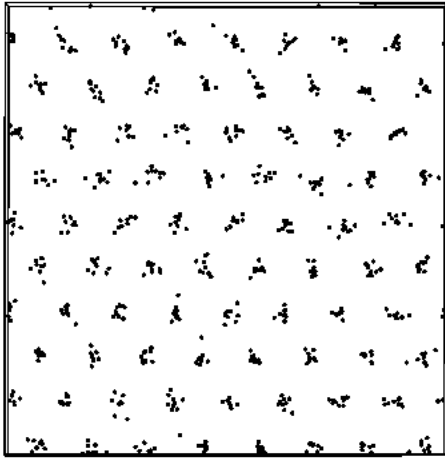


FIG. 8. R. Blaak, Journal of Chemical Physics

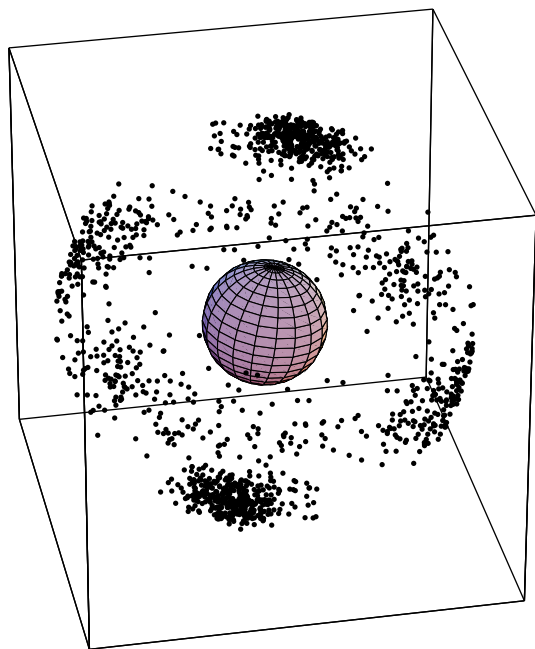


FIG. 9. R. Blaak, Journal of Chemical Physics

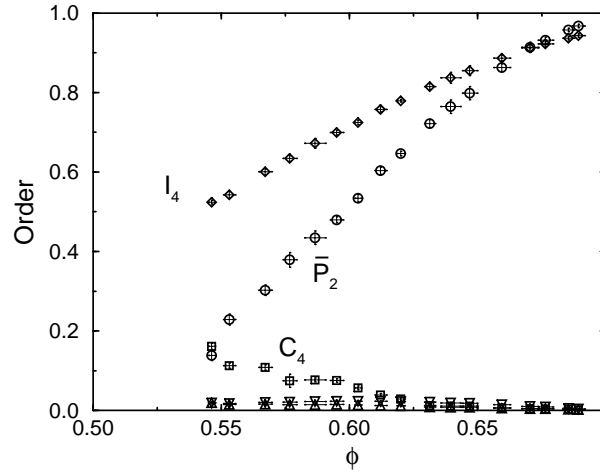


FIG. 10. R. Blaak, Journal of Chemical Physics

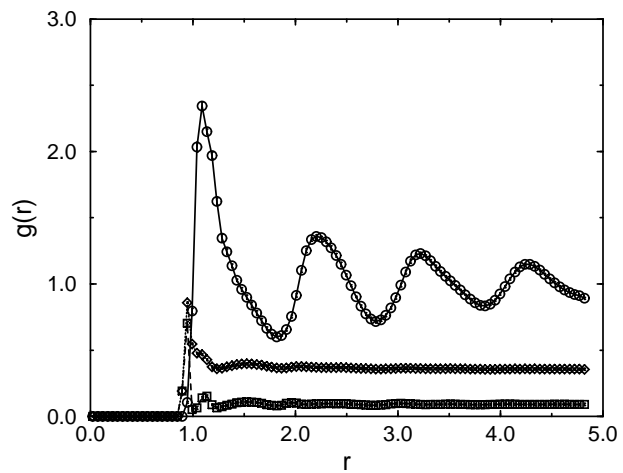


FIG. 11. R. Blaak, Journal of Chemical Physics

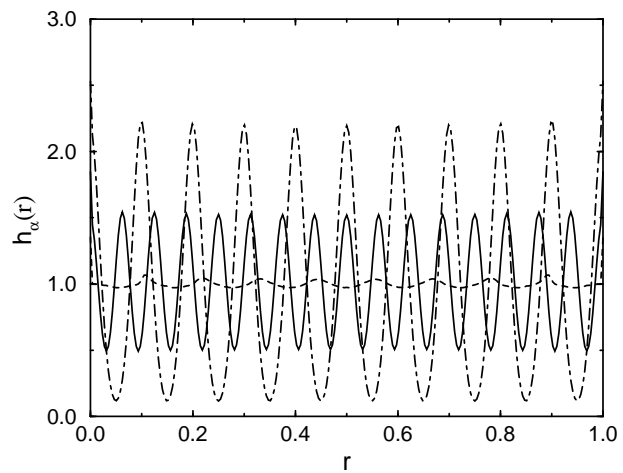


FIG. 12. R. Blaak, Journal of Chemical Physics